12. Способ получения гранулированного титансодержащего цеолита: Пат. 2422360 РФ. № 2010100533/05, заявл. 11.01.2010, опубл. 27.06.2011. Бюл. № 18.
13. *Данов С.М., Сулимов А.В., Овчаров А.А., Сулимова А.В.* Влияние условий приготовления титансодержащего цеолита на его каталитическую активность в процессе эпоксидирования олефинов пероксидом водорода // Катализ в промышленности. 2011. № 1. С. 30—36.
14. Технология катализаторов / Под. ред. И.П. Мухленова. Л: Химия, 1989. 272 с.
15. *Боресков Г.К.* Гетерогенный катализ. М: Наука, 1986. 303 с.
16. *Айлер Р.* Химия кремнезема. Т. 1—2. М: Мир, 1972. 1128 с.
17. *Дзисько В., Карнаухов А., Тарасова Д.* Физико-химические основы синтеза окисных катализаторов. Новосибирск: Наука, 1978. 384 с.
18. Способ грануляции адсорбентов: А.С. 196718, № 1063345, опубл. 01.01.1967.
19. *Сычев М.* Неорганические клеи. Л: Химия, 1986. 152 с.
20. Method for producing a shaped body using a metal oxide sol: Пат. 6551546 США. № 20000646902, заявл. 10.10.2000, опубл. 22.04.2003.
21. Способ получения пропиленоксида: Пат. 2332409 РФ. № 2005138058/04, заявл. 10.05.2004, опубл. 27.08. 2008.
22. *Тарасова Д., Дзисько В., Гусева М.* Влияние условий получения на удельную поверхность катализаторов и носителей. Ч. 1. Силикагель // Кинетика и катализ. 1968. Т. 9. № 5. С. 1126—1133.
23. Process for the production of a titanium silicalite shaped body: Европейский пат. 1268057. № 20010915393, заявл. 21.03.2001, опубл. 02.01.2003.
24. *Исмагилов З.Р., Шкрабина Р.А., Корябкина Н.А.* Алюмооксидные носители: производство, свойства и применение в каталитических процессах защиты окружающей среды. Аналит. обзор. Новосибирск: Ин-т катализа им. Г.К. Борескова СО РАН, 1998. 82 с.
25. *Исмагилов З., Шкрабина Р., Корябкина Н.* Алюмооксидные носители: производство, свойства и применение в каталитических процессах защиты окружающей среды. Аналит. обзор, Сер. «Экология». Новосибирск, 1998. 50 с.
26. *Мухленов И.П., Добкина Е.И., Дерюжкина В.И., Сороко В.Е.* Технология катализаторов. Л: Химия, 1989. 272 с.

UDK 547.1-32:662.74

HUMIC ACID-Fe AS CATALYST FOR COAL LIQUEFACTION

© 2013 г. **Qindao Wang**[1], **Haoping Wang**[2], **Jun Jin**[2]

[1] Vocational and Technology College, Liaoning Shihua University, Fushun, Liaoning, P. R. China

[2] Department of Chemistry, School of Chemistry and Materials Science, Liaoning Shihua University, Fushun, Liaoning, P. R. China

1. Introduction

The catalysis of iron compounds in the coal liquefaction reaction has been known for a long time. The Germans (Friedrich Bergius at 1913 that led to a Nobel Prize in chemistry in 1931) found that adding iron to the feed slurry could improve the liquefaction of coal. In certain cases the addition of sulfur to the system could further promote the effect of the iron. Stoichiometry indicated that iron sulfide (FeS) was the ultimate form of the iron in the liquefaction residue. With the advent of X-ray diffraction technique it was confirmed that iron existed as pyrrhotite that is widely considered to be an active phase in coal liquefaction [1—3].

It has been reported that smaller particle size of iron based catalyst precursor was beneficial to increasing the

Wang Qindao *– lecturer of Vocational and Technology College, Liaoning Shihua University, Fushun, Liaoning, P. R. China. Ph: +86-24-56863325. E-mail: wangqingdao@yahoo.com*

Wang Haoping *– Professor of Department of Chemistry, School of Chemistry and Materials Science of the same university. Ph: +86-24-56863325. E-mail: whp-a@163.com*

Jin Jun *– Professor of the same department. Ph: +86-56863325. E-mail: jinjun1956@163.com*

catalytic performance [4]. Takao Kaneko et al. present the effect of the highly dispersed γ-FeOOH catalyst on the direct liquefaction of coal. They demonstrate an excellent catalytic activity of highly dispersed γ-FeOOH catalyst for the direct liquefaction of low-rank coal [5]. Liu et al. [6] have developed a so-called *in situ* impregnated iron sulfide catalyst by mixing a coal-containing Na_2S solution with a $FeCl_3$ solution to produce nano-sized iron sulfides and then precipitate on coal surface. Afterward, they modified *in situ* impregnation method and confirmed that the active phase of catalysts existed mainly as nano-scale γ-FeOOH and FeS, or possibly of Fe/O/S [7].

In recent years, there has been renewed interest in the use of iron-based catalysts for direct coal liquefaction (DCL) because of not only their low cost, environmental friendliness and being disposable, but also their high activity to be competitive with more expensive and nondisposable catalysts in terms of both total conversion and oil yields.

It is well known that carboxylic group (—COOH) bonded to polyaromatic cluster exists dominantly in low-rank coals, and uni- and divalent metal cations can easily exchange proton with —COOH. The catalytic effects of exchanged cations on the liquefaction of coals had been discussed, and it was well recognized that catalysts containing Fe^{2+}, Ni^{2+} and Co^{2+} exhibited excellent activity for hydrogenolysis reaction of crude oil or coal [8—12]. However, from the viewpoint of the industrial production, the above-mentioned catalytic method is hardly feasible to be used for liquefaction of coal. Li et al. proposed an inexpensive, highly active and disposable iron-based catalyst with the iron content of 1—15 wt.%, consisted of the active phase of γ-FeOOH, the carrier of liquefied coal and some impurities as well as water, prepared by *in situ* impregnation method [13].

Coal can serve as the support of the iron-based catalyst by ions exchange or impregnation process, which is attributed to the presence of humic acid (HA) in low-rank coals. HA is one of the major components of humic substances which are dark brown and major constituents of soil organic matter humus that contributes to soil chemical and physical quality and are also precursors of some fossil fuels. HA, a chemically heterogeneous compound, possesses various types of functional groups in different proportions and configurations, such as carboxyl (–COOH), amine ($–NH_2$) and hydroxyl (–OH), and a negative charge in weakly acidic to basic media resulted from deprotonation. The predominant functional group in HA is hydroxyl including phenolic hydroxyls and alcoholic hydroxyls, with the help of which these molecules can chelate positively charged multivalent ions, such as Mg^{2+}, Ni^{2+}, Co^{2+} and Fe^{2+}. The chelate compounds obtained are able to act as the catalyst for coal liquefaction reaction. The objectives of this paper are two-fold. The first one is to develop active disposable catalyst which is the chelate compounds of iron with humic acid, and would be suitable for coal liquefaction reaction. The second objective is to validate its catalytic activity and preliminary characterized of the catalyst.

2. Experiments section

2.1. Materials

2.1.1. Coals

Coals were sampled from ten different zones in China. Each of them belongs to one of brown coal, long flame coal and bituminous coal, respectively. The elemental and proximate analyses results of the coals are shown in Table 1. The coal sample was ground to less than 75 μm and stored under N_2 atmosphere before use. Humic acid used in this work is from Neimenggu (China). The composition analysis results of humic acid are provided in Table 2.

2.1.2. Oil

The crude oil was sampled from Shengli oilfield, and the vacuum residue was from Liaohe oil refinery. Proximate and ultimate analyses results are shown in Table 3.

2.1.3. Catalysts

Both Fe_2O_3 and FeS used in this work are the reagents with chemical pure. HA-Fe catalysts were prepared by using $FeSO_4$ and HA with different ratio as starting materials. Two-line ferrihydrite was prepared by using the method proposed by Zhao et al. [14]. An appropriate amount of ammonium hydroxide was added to 1 liter of 0.1M $Fe_2(SO_4)_3$ solution until the pH reached 10. The reddish brown precipitate was filtered, and the cake obtained was dried at 50 °C in oven and then ground into fine powder.

2.2. Characterization of HA and HA-Fe

2.2.1. Purification of HA

Briefly, HA was extracted from the sample with 0.1 $mol \cdot dm^{-3}$ NaOH at 1 : 10 solid to solution (mass/volume) ratio under N_2 for 4 hours. The suspension was then centrifuged at 4500 $r \cdot min^{-1}$ for 30 min, the supernatant was acidified with 6 $mol \cdot dm^{-3}$ HCl to pH 1.0. Precipitated HA was separated. In order to minimize the ash content, this procedure was repeated three times.

Table 1
Proximate and ultimate analysis of coals used in this work

Coal	Proximate analysis*			Ultimate analysis				
	M_{ad}, %	A_d, %	V_{daf}, %	C_{daf},%	H_{daf},%	N_{daf},%	S_{daf},%	O_{daf},%
Fushun	2.28	7.33	42.06	81.16	5.64	1.27	0.49	11.44
Huadian	8.20	6.83	47.0	73.39	5.66	1.84	0.40	18.71
Tongchuan	3.12	8.65	31.16	83.05	5.46	1.27	0.65	9.57
Yilan	1.63	9.86	49.00	78.23	6.04	1.44	0.22	14.06
Shulan	8.05	14.79	52.51	72.67	6.00	1.88	0.26	19.19
Yuanbaoshan	4.10	8.58	45.86	74.78	4.75	0.90	1.03	18.54
Meihekou	5.70	5.93	45.96	74.02	5.78	1.83	0.44	17.93
Pingchuan	7.72	5.58	43.25	73.86	5.50	1.26	1.14	18.24
Xifen	3.73	6.17	45.52	76.21	6.10	1.52	0.56	15.61
Baicheng	15.86	8.46	42.47	73.23	4.53	1.00	0.40	20.84

* M_{ad} and A_d are moisture and ash in air dried sample, respectively; V_{daf} – volatile matter in dry ash free (DAF)

Table 2
Ultimate analysis of HA catalyst used in this work

Element	C	H	S	N	O	Na	Mg	Al	Si	P	K	Ca	Ti	Mn	Fe	Sr
Wt.%	40.14	4.06	2.92	1.03	26.72	0.10	0.30	2.40	6.75	0.12	0.26	3.58	0.12	0.05	0.82 (10.60*)	0.06
* This is the iron content in HA-Fe																

Table 3
Properties of heavy oil and vacuum residuum

Property	Heavy oil	Vacuum residuum (*Vr*)
Density (20 °C), g/cm^3	0.95	1.03
Viscosity (100 °C), cSt	94	1350
Moisture, wt.%	6.0	trace
Total sulphur content, wt.%	1.58	0.35
Ash, wt.%	0.53	0.61
Carbon residue (Con), wt.%	8.29	16.0
Mechanical impurities (m/m), %	0.86	–
Fraction range, °C	–	> 540

2.2.2. The total cation exchange capacity of HA

In a glass flask 0.2M NaOH solution (20 ml) was added to depurative HA (10 mg). Also, a same volume of 0.2M NaOH without HA was prepared as a blank solution. The flask was carefully shaken for 24 h at room temperature. Then, the suspension was filtrated centrifugally by 0.45 mm membrane filter (Millipore) at 3000 r·min^{-1} for 15 min, and the residue was washed with double distilled water. Potentiometric titration of filtrate and the washing solution was carried out with 0.1M HCl up to pH of 7.0. The total cation exchange capacity (CEC_t, meq/g), can be expressed as:

$$CEC_t = (V_b - V_s)N/W,$$

where V denotes a solution volume for titration to the sample (V_s) and blank (V_b), ml; N — normality of acid; W — weight of the sample, g.

2.2.3. Carboxyl and Phenolic groups

We added 10 ml of 0.2M $(CH_3COO)_2Ca$ solution to 10 mg of depurative HA. After the same shaking, centrifugation, filtration and washing processes as above-mentioned those, the solution was titrated with 0.01M NaCl + + 0.09M $NaClO_4$ up to pH of 9.8. The cation exchange capacity of carboxyl groups (CEC_c, meq/g) is expressed as:

$$CEC_c = (V_s - V_b)N/W.$$

For phenolic groups, the corresponding value can be calculated by the equation of $CEC_p = CEC_t - CEC_c$.

2.2.4. FT-IR and XRD characterization

FT-IR spectroscopy is useful in the gross characterization of humic compounds for the detection of structural changes caused by chemical modifications and to ascertain and characterize the formation of metal humate complexes. FT-IR spectra of HA-Fe were recorded on KBr pellets (1.0 mg of HA-Fe and 150.0 mg of KBr) using a Perkin-Elmer Spectrum^{TM} GX, FT-IR spectrophotometer.

Japanese Rigaku Dmax-rA X-ray diffractometer with Ni-filtered CuKα radiation is adopted to ascertain the crystal structure of the ferric oxyhydroxides in the HA-Fe.

2.3. Reaction procedure of coals conversion

2.3.1. Dewatering of coals and heavy oil

The coal powder and heavy oil (or residual oil) firstly blended according to a certain percentage in heated reactor equipped with agitator and condensing apparatus. The optimum experiment conditions were found as follows: the temperature of 160 °C and agitation speed of 500 r·min^{-1}. The volatile components and water of the coal and oil were vaporized and subsequently condensed. Thus the water is easily separated from the oil by decantation. Afterwards, the coal-oil mixture was fed into next process.

2.3.2. Co-processing of coal and oil

The reactor is autoclave with agitator. The autoclave was equipped with a cooling coil through which cold water could be passed to reduce the temperature if desired. The temperature of the reactants was continuously monitored.

The liquid products were divided into soluble and insoluble moieties by a Soxhlet extraction method successively using THF, toluene and *n*-hexane as solvents. The total conversion was defined by the percent of converted into THF-soluble compounds. THF-soluble and toluene-insoluble fractions were defined as preasphaltenes, while toluene-soluble and hexane-insoluble fractions were defined as asphaltenes. The percent of converted into hexane-soluble compounds defined as oil yield.

2.4. The analysis of the products from co-liquefaction

The gasoline fraction, diesel fraction, VGO fraction and residue fraction were determined by gas chromatography — mass spectrometric method (HP 6890 GC/HP 5973MS, and HP GC2MSD Workstation). The capillary chromatogram column: 40 m × 0.25 mm; Fischer 500 5 s distillation apparatus (Germany); the carrier gas was nitrogen.

Polycyclic aromatic hydrocarbons were determined by GC-MS total ion current chromatogram analysis using 6890/5973N GC-MS Agilent Technologies. Aromatic hydrocarbons are separated from liquefaction products According SY/T 5119-2008 [27]. HP-5 capillary chromatogram column, 60 m × 0.25 mm; the carrier gas was helium, 1 ml/min; splitless inlet. Temperature program: initial temperature 100 °C and the temperature rose to 320 °C when heating rate was 3 °C/min.

3. Results and discussion

3.1. Characterization results of HA

The CEC values of the HA obtained are: CEC_t = 7.03, CEC_c = 4.81 and CEC_p = 2.21. During the interaction of Fe^{2+} ions with HA, two types of complexes, ionic and non-ionic ones, were formed. The carboxyl and phenolic hydroxyl groups are responsible for the formation of ionic complexes, and the formation of non-ionic complexes involves the carboxyl and carbonyl (keto) groups. Using the method specified by Baruah et al. [15], the distribution ratio of iron in Fe^{2+} complexes, prepared at pH of 8, is ionic Fe/non-ionic Fe = 55 : 45 (wt./wt.).

These results show that a substantial fraction of the mass of the humic acids is in carboxylic acid functional groups, which endow these molecules with the ability to chelate (bind) positively charged multivalent ions. This chelation of ions is probably the most important role of humic acids played with respect to catalysis for coal liquefaction.

3.2. The FT-IR spectrum of HA-Fe

The FT-IR spectrum of HA-Fe (Fig. 1) exhibits the typical major peaks for humic acid: OH stretching vibration and possibly NH stretching vibration (3300—3500 cm^{-1}), two distinct peaks at 2922 and 2852 cm^{-1}

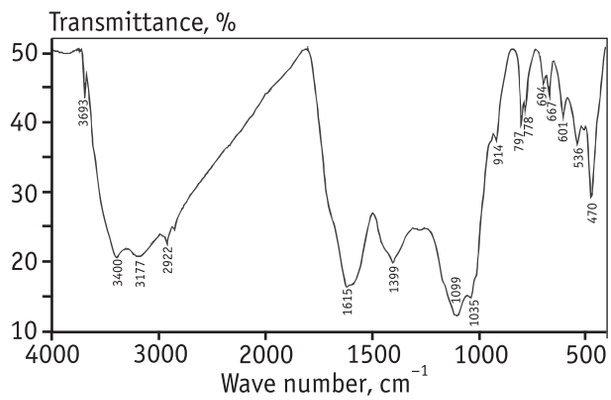

Fig. 1. Fourier transform infrared spectra of humic acid-Fe

(C—H asymmetric vibration, C—H stretching vibration of —CH), aromatic C=C stretching vibration and/or symmetric —COO— stretching vibration (1600—1650 cm^{-1}), —OH and —CO deformation vibration from alcoholic and phenolic —OH and/or —COO— anti-symmetric stretching (1385 cm^{-1}), and —CO stretching vibration and —OH bending vibration of —COOH (1200—1220 cm^{-1}).

Generally, the most important characteristic of the IR spectra of HA is the absorption peak at about 1700 cm^{-1} that assigned to C=O stretching vibration. Reaction between metal ion and —COOH functional groups, forming the metal ion complex, results in the disappearance of the absorption band at 1700 cm^{-1} and the appearance of new bands at about 1600 cm^{-1} (symmetric COO— stretching vibration) and 1385 cm^{-1} (antisymmetric COO— stretching vibration). The disappearance of this band also suggests that most of the —COOH groups were converted to the COO— groups [16].

About iron configuration in the catalyst, may be the mixture of γ-FeOOH, α-FeOOH and ferrihydrite. The characteristic absorption peaks of γ-FeOOH locate at wave number = 1150, 1022, 744 and 468 cm^{-1}, and the peaks at wave number are 888, 795, 625 cm^{-1} belong to α-FeOOH [17—18]. In Fig. 1 the peaks at wave number are 1, 470, 1035 cm^{-1} and 914, 797 cm^{-1} ought to be the characteristic absorption ones of γ-FeOOH and α-FeOOH respectively. However the absorption peaks at wave number 1150 cm^{-1} are not clearly observed in the present spectra. This is because the absorption regions for sulfate and silicate seem to overlap over the main absorption peaks of γ-FeOOH. And sulfate may come from $FeSO_4$, which was used for the synthesis catalyst, and silicate is a component of ash in HA. There exist many functional groups and foreign ions nearby FeOOH, so influence on absorption peaks is inevitable. The displacement and cover of adsorption peaks occur usually.

Lepidocrocite (γ-FeOOH) appears to be thermodynamically metastable with respect to goethite (α-FeOOH), and yet the former phase still can form and exist both in nature and laboratory. In simple terms, in laboratory preparative methods of the γ-FeOOH and α-FeOOH are presented as follows:

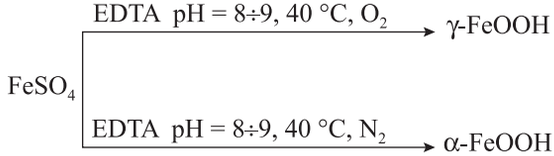

If air was used, a mixture of γ-FeOOH and α-FeOOH can be obtained. If EDTA is replaced by HA with the ability to chelate, a mixture of γ-FeOOH and α-FeOOH also may be obtained. In other words, the preparative method of HA-Fe is similar to that of lepidocrocite and goethite. Therefore, there exists FeO_6 octahedron structural unit (FeOOH) in HA-Fe. However, the structure and morphology changed while the linkage of FeO_6 octahedral units in γ-FeOOH and α-FeOOH was considerably distorted by the incorporation of the other anions, such as $—SO_4^{-2}$ and humate radical. Meanwhile, the intensities of the corresponding absorption peaks of γ-FeOOH and α-FeOOH decreased.

Ferrihydrite (Fh) is a widespread hydrous ferric oxyhydroxide. Fh only exists as a fine grained and highly defective nanomaterial. The XRD pattern of Fh contains two broadening characteristic diffraction peaks in its most disordered state, and a maximum of six strong diffraction lines in its most crystalline state. The principal difference between these two diffraction end-members, commonly named two-line and six-line ferrihydrites, is the size of the constitutive crystallites. The characteristic absorption peaks in IR spectra of six-line Fh in 500—4000 cm^{-1} range are marked as A, B, C, D, E and F and the corresponding wave numbers are 870, 1365, 1493, 1650, 3400 and 3700 cm^{-1}, respectively [19—20]. Fig. 1 shows that E-line and F-line can be identified clearly, and 1615 cm^{-1} should be ascribed to D-line.

3.3. XRD characterization of the HA-Fe and HA

Fig. 2 and Fig. 3 show the XRD patterns of HA-Fe and HA, respectively. The pattern in Fig. 2 revealed that there exist two iron oxide/oxyhydroxides and clay impurity in the HA-Fe. The iron oxide/oxyhydroxides are α-FeOOH and three-line Fh. The results are in good agreement with that of FT-IR analysis, but pattern of γ-FeOOH is not discovered, indicating that it may exists as highly dispersion or amorphous state.

The formula of ferrihydrite was expressed in various forms, such as $5Fe_2O_3 \cdot 9H_2O$, $Fe_5HO_8 \cdot 4H_2O$ and

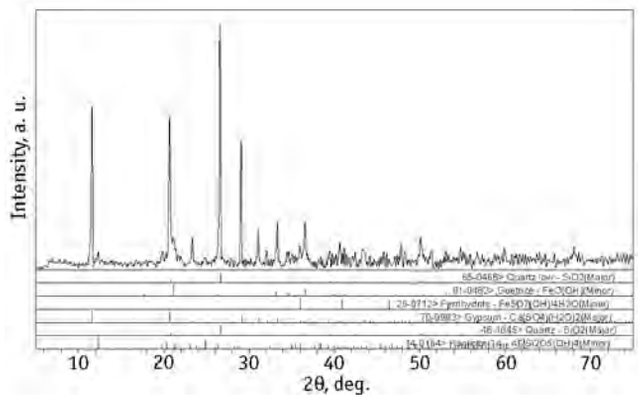

Fig. 2. X-ray diffraction pattern of humic acid-Fe

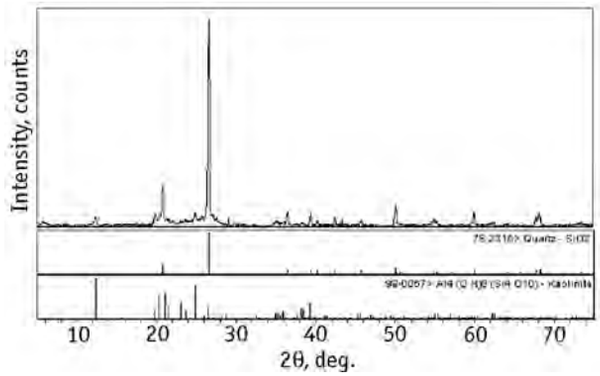

Fig. 3. X-ray diffraction pattern of humic acid

$Fe_2O_3 \cdot 2FeOOH \cdot 2.6H_2O$ [20—22]. These formulae are essentially equivalent and can be reduced to $FeOOH \cdot 0.4H_2O$. The average crystallite size of Fh is unusually small (~3 nm). Because of its reactivity and large specific surface area (> 200 m^2/g), it had been studied as a catalyst for a number of reactions, identified as amorphous FeOOH [23]. In this work, the catalytic performance of Fh as a catalyst for coal liquefaction was investigated and the results are shown in Table 4.

By comparison in Fig. 2 and Fig. 3, it is found that the diffraction patterns of the HA-Fe and HA are dissimilar. Fig. 3 shows that there is no crystalloid of Fh or α-FeOOH, there is only SiO_2 and kaolinite here.

Ultimate analysis indicates that there exist Ti, Mn, Sr etc. metals, which roles in catalytic liquefaction of coal should not be neglected. A highly purified HA, de-iron and other trace metals (Fe ≤ 0.05 wt.%), were used to prepare HA-Fe catalyst. The results showed that it is not as good as the original ecology humic acid.

Humic acids are heterogeneous macromolecules derived from chemical, physical and biochemical degradation of organic matter. Their significance comes from the ability to bind and mobilize metals and anthropogenic organic contaminants. It has been observed that, under certain conditions, the interactions between humic acid and iron in the presence of sulfur-donating species are important in the accumulation of various forms of sulfur in coal. The test results indicate that (see Table 2) the iron content of humic acid is approximately 0.8 wt.%. Apparently, the iron in HA is in amorphous state. As a catalyst, their contents are too low.

3.4. Dewatering process

In this work, we use mainly low-rank coal, such as brown coals and small amount of bituminous coal. Brown coals are important energy resources in the near future because of their abundant deposits. But dewatering (drying) process is necessary prior to use for its liquefaction because their water content is very high, and even reach as high as 60 % by weight for some coals. Current dewatering technology of low-rank coal prior to liquefaction is mainly evaporation drying, resulting in a direct loss of the heat of evaporation (~2.3 MJ/kg). Therefore, development of an efficient dewatering process is desired for more utilization of brown coals, especially for the hydro-liquefaction of brown coals. In earlier work [24], we had proposed a method similar to non-evaporating drying process (see 2.3.1). In this process, brown coals are treated under hydrothermal conditions at ~200 °C, where upgrading as well as dewatering of brown coals can be realized through the decomposition of oxygen-containing functional groups. This process has several advantages:

1) the method is more effective than evaporation drying. For example, when Shulan brown coal whose water content was 15 wt.% was treated by heavy oil at 150 °C, the water content can be reduced to less than 1 wt.%;

2) there was not water or only trace water in gas products of hydro-liquefaction. So, the adverse influence of water vapor on reaction pressure greatly reduced;

3) in the process, the interaction between coal and heavy oil may breach the crosslink among hydrogen bonds in coal. On the contrary, new hydrogen bonds between oil and coal are formed, which lead to swelling of coal particles with the pore diameter expanding. This is helpful to the coal liquefaction.

3.5. Development of disposable catalysts

3.5.1. Comparison of catalytic performance

The equipments of the reaction see 2.3.2. After air was displaced, the cold H_2 pressure was then raised to the prefixed values (cool H_2 pressure is chosen as 3, 5 or 8 MPa). The reaction mixture was heated to the desired temperature and then was maintained for 1.0—1.5 hour, and the whisk speed was set at 500 $r \cdot min^{-1}$. Afterwards, heat supply to the reactor was shut off. Gases were collected and analyzed. Experiments were carried out in at least duplicate, in many cases, four replicates were used.

To establish the beneficial effects of the catalyst, test runs were conducted without catalyst, and with iron oxide (Fe_2O_3) plus FeS catalyst and ferrihydrite (two-line) catalyst, respectively. It was anticipated that the activity of iron catalyst (Fe_2O_3, FeS) would be lower than present catalyst HA-Fe and to compensate for this a much larger amount of iron catalyst was used. The detailed reaction conditions see in Table 4.

The results of the comparison are summarized in Table 4. The addition of catalysts resulted in a dramatic in-

crease in the conversion. Total conversion (THF-soluble) and hexane-soluble compounds (oil yield) without the addition of catalyst were 48.9 % and 30.1 %, respectively. The total conversion and hexane-soluble increased to 78.2 % and 50.6 % with iron catalyst and increased further with the HA-Fe catalyst to 88.2 % and 64.3 %, respectively.

Table 4 clearly shows that the HA-Fe catalyst gave significantly higher conversions under the same reaction conditions. It can therefore be concluded that HA-Fe catalyst has better catalytic performance for coal liquefaction. In addition, Table 4 shows that Fh as catalyst exhibited the quite high activity for coal liquefaction, which was hardly reported in open literatures yet.

Hydrogen consumption is also an important comparison factor of catalytic performance for coal liquefaction. As shown in Table 4, the hydrogen consumptions without catalyst and with the HA-Fe catalyst are 1.7 % and 1.8 %, respectively. However, the percents increase to 2.7 % and 3.0 % when used iron catalyst and Fh catalyst, respectively. This higher hydrogen consumption yields a liquid with higher hydrogen content and a lower THF insoluble content.

3.5.2. The analysis of the oil for co-liquefaction

Tongchuan coal and residual oil was selected as feedstock for co-processing. As a comparison, the hydroliquefaction of the residual oil was carried out. Reaction conditions were basically the same as that in Table 4, but oil/coal = 2 : 1 (wt./wt.). Three hydrogenation reaction samples were analyzed by RIPP (Research Institute of Petroleum Processing of SINOPEC). The samples properties of the total liquid product are summarized in Table 5.

As shown in Table 5, two systems tested at the different reaction temperatures: 420 and 440 °C, but both have higher oil yield. A primary goal of catalyst development for direct coal liquefaction is to maximize the yield of distillate products while minimizing the conversion to by-product of hydrocarbon gases which unprofitably consume much of the hydrogen.

Table 5 clearly shows that the yield of gasoline fraction (8.75 %) and diesel distillate (54.84 %) is 63.59 % at 420 °C, but it decreased to 55.89 % (7.92 % + 47.97 %) at 440 °C. This is theorized to be due to thermal degradations that produce coke and light gases. Therefore, the better reaction temperature is 420 °C. On the residual oil, the oil yield, including gasoline and diesel, has only 45.60 %, and cut fraction (> 500 °C) is beyond 16.00 %. This means that the quality of the liquid products is improved by coal/oil synergies in co-processing. However, the components of hexane-soluble liquids are complex, the quality of the oil are still far away from the standard, which need to be further refined.

Table 4

Co-liquefaction of Tongchuan coal and vacuum residuum* with and without catalyst**

Catalyst	THF soluble (daf), %	Oil yield (daf), %	H_2 consumption, wt.%
–	48.9	30.1	1.7
HA-Fe (0.8 %)	88.2	64.3	1.8
Fe_2O_3 + FeS 3 % + 2 %	78.2	50.6	2.7
Ferrihydrite (two-line 1.5 wt.%)	91.4	65.5	3.0

* Concentrated of coal 43.7 %.
** Operating conditions: temperature – 420 °C; cool H_2 pressure – 8.0 MPa; reaction time – 90 min

Table 5

Product distribution for hexane-soluble liquids

Products	Reaction parameters		
	*Vr/T**, % (420 °C)	*Vr/T*, % (440 °C)	*Vr*, % (440 °C)
Component			
alkanes	19.10	19.90	11.10
total cyclane	32.10	25.10	28.00
mononuclear aromatics	15.80	15.10	15.70
bicyclic aromatics	11.50	12.40	13.90
tricyclicaromatics	3.30	4.50	5.30
tetracyclic aromatics	1.70	2.70	3.70
pentacyclic aromatics	0.20	1.00	1.30
unidentified alkylbenzene	0.80	1.10	1.70
thiophene	2.30	2.10	2.10
gum	13.20	16.10	17.20
Distillation range			
gasoline fraction (IBP–180 °C)	8.75	7.92	7.47
diesel distillate (180–350 °C)	54.84	47.97	38.13
distillation cut (350–500 °C)	29.30	38.38	37.89
distillation cut (> 500 °C)	7.11	5.73	16.51

* *Vr* is short for vacuum residuum, *T* is short for Tongchuan bituminous coal

3.6. Reactivity screening test for various coals

Ten different coals, heavy oil, and one original ecology HA were evaluated during this screening test. The general properties of the coals, the heavy oil and HA used in the test are summarized in Tables 1, 2 and 3, respectively. The

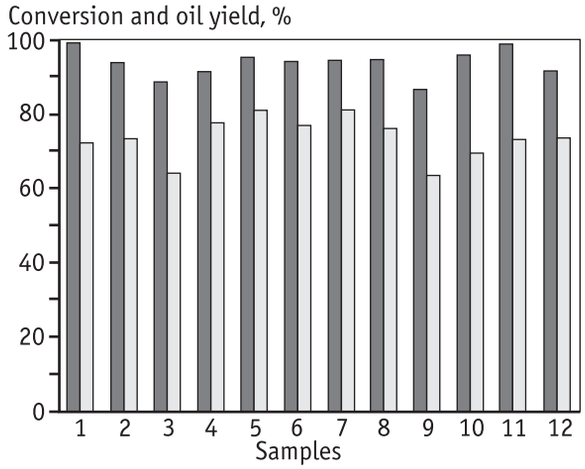

Fig. 4. The total conversion (dark bars) and oil yield (light bars)

Coals: *1* – Huadian (L); *2* – Shulan (L); *3* – Tongchuan (B); *4* – Yuanbaoshan (L); *5* – Pingzhuang (L); *6* – Baicheng (L); *7* – Xifeng (L); *8* – Meihekou (L); *9* – Fushun (S); *10* – Yilan (S).
Humic acid: *11*. Heavy oil: *12*
L – lignite, B – bitumite, S – sub-bituminous

operating conditions used during reactivity test are given as follows:

heavy oil/coal ratio, wt./wt. .....2 : 1

pressure of cool H_2, MPa 8

temperature, °C 420

residence time, h 1

Fe in catalyst HA-Fe, wt.% 0.5

The product yields on the coal-oil co-processing using HA-Fe catalyst are shown in Fig. 4. The maximum total conversion of coal-oil is 99.00 %, while the minimum one was 91.30 %. For the oil yield, the highest is 80.70 %, the lowest one is 63.50 %. By comparison with Table 4 it is found that the conversion and oil yield is higher than that of Tongchuan coal.

The results in Fig. 4 show that the best coals are Huadian coal and Yilan coal in terms of the total conversion or oil yield. This may be expressed that, the higher H/C molar ratio is, the better hydrogenation effect is. H/C molar ratios of Huadian coal and Yilan coal are 0.926 and 0.925, respectively. HA, as a precursor of coal, its conversion and oil yield are 98.68 % and 73.00 %, respectively. However, its ash is too high.

4. Conclusion

Recently, research on increasing the activity of iron based catalysts focuses on decreasing the particle size, increasing catalyst dispersion. Catalysts with highly dispersed active phase, such as iron, can significantly influence conversion of coal in liquefaction [2]. It was widely recognized that a highly dispersed catalyst can be superior to a supported catalyst, because the dispersed catalyst has a close contact with the surface of coal particle, which facilitates the activation and transfer of hydrogen to the coal-derived fragments and reactive sites. Accordingly, finer particles and a higher dispersion of the catalyst species would lead to a higher catalytic activity [5]. Humic acid is partly dissolved in water and complete miscibility with heavy oil, resid etc. solvents, their macromolecules radii can range from 6 to 50 nm, the range of molecular mass (number average molecular weight) is at $9 \cdot 10^3$—$50 \cdot 10^3$ [25—26]. Fe^{2+} or Fe^{3+} dispersed finely into the HA matrix through the ion exchange with —COOH groups or chelation with carbonyl group in humic acid macromolecules. Therefore, Fe in HA-Fe exists in a highly dispersed state, which is responsible for the high catalytic activity in DCL.

The characterization results showed that Fe presents in HA in various forms, such as α-FeOOH, ferrihydrite (three-line) and amorphous Fe. In this work, the results of co-liquefaction using HA-Fe catalyst showed distinctly that HA-Fe was more effective catalyst than usual iron pyrite. In addition, the optimization of process of co-liquefaction has been done.

The financial support received from SINOPEC (No. 108106) is greatly appreciated. The authors would like to thank RIPP of SINOPEC for assistance in acquisition of analytic results for Tables 2 and 5. We are indebted to Prof. Jiang Heng and Chu Gang for assistance in IR spectrum and X-ray diffraction.

References

1. *Cugini A.V., Krastma D., Lett R.G., Balsone V.D.* // Catal. Today. 1994. Vol. 19. P. 395—407.
2. *Derbyshire F., Hager T.* // Fuel. 1994. Vol. 73. P. 1087—1092.
3. *Mochida I., Sakanishi K.* // Adv. in Catal. 1994. Vol. 40. P. 39—85.
4. *Darab J.G., Linehan J.C., Matson D.W.* // Energy & Fuels. 1994. Vol. 8. P. 1004—1005.
5. *Kaneko T., Tazawa K., Okuyama N., Tamura M., Shimasaki K.* // Fuel. 2000. Vol. 79. P. 263—271.
6. *Liu Z., Yang J., Zondlo J.W., Stiller A.H., Dadyburjor D.B.* // Fuel. 1996. Vol. 75. P. 51—57.
7. *Jisheng Zhu, Jianli Yang, Zhenyu Liu, Dady B Dadyburjor, Bing Zhong, Baoqing Li* // Fuel Processing Technology. 2001. Vol. 72. P. 199—214.

8. *Sugano M., Mashimo K., Wainai T.* // Fuel. 1999. Vol. 78. P. 945—951.
9. *Taghiei M.M., Huggins F.E., Ganguly B., Huffman G.P.* // Energy & Fuels. 1993. Vol. 7. P. 399—405.
10. *Taghiei M.M., Huggins F.E., Mahajan V., Huffman G.P.* // Energy & Fuels. 1994. Vol. 8. P. 31—37.
11. *Sugano M., Suzuki K., Ohki-Ikemizu R., Mashimo K.* // Chem. Eng. Trans. 2009. Vol. 18. P. 683—688.
12. *Sugano M., Hirano K., Mashimo K.* // Ind. Eng. Chem. Res. 2010. Vol. 49. P. 1138—1142.
13. Patent CN1778871A China / W.B. Li, G.P. Shu, K.J. Li. 2006.
14. *Zhao J., Hugging F.E., Zhen Feng, Huffman G.P.* // Clay & Clay Minerals. 1994. Vol. 42. P. 737—746.
15. *Baruah M.K., Upreti M.C., Baishya N.K., Dutta S.N.* // Fuel. 1981. Vol. 60. P. 971—974.
16. *Erdogan S., Baysal A., Akba O., Hamamci C.* // Polish J. of Environ. Study. 2007. Vol. 16. P. 671—675.
17. *Kwon S.-K., Shinoda K., Suzuki S., Waseda Y.* // Corrosion Sci. 2007. Vol. 49. P. 1513—1526.
18. *Kwon S.-K., Suzuki S., Saito M., Waseda Y.* // Corrosion Sci. 2005. Vol. 47. P. 2543—2549.
19. *Seehra M.S., Roy P., Raman A., Manivannan A.* // Solid State Comm. 2004. Vol. 130. P. 597—601.
20. *Russell J.D.* // Clay Minerals. 1997. Vol. 14. P. 109.
21. *Towe K.M., Bradley W.F.* // J. Colloid and Interface Sci. 1967. Vol. 24, P. 384—392.
22. *Fleischer M., Zhao G.Y., Kate A.* // Am. Mineral. 1975. Vol. 60. P. 485.
23. *Liaw B.J., Cheng D.S., Yang B.L.* // J. of Catal. 1989. Vol. 118. P. 312—326.
24. *Chun-Zhu Li.* Advances in the Science of Victorian Brown Coal. Elsevier, 2004. Chinese edition, 2009. 319 p.
25. *Stevenson F.J.* Humus Chemistry: Genesis, Composition, Reactions. Second ed. John Wiley & Sons: New York, 1994. 512 p.
26. *Kawahigashi M., Sumida H., Yamamoto K.* // J. Colloid and Interface Sci. 2005. Vol. 284. P. 463—469.
27. SY/T 5119-2008 (Chinese). Analysis method for fractions of rock extract and crude oil. Petroleum Industry Press: Beijing, China, 2008.

УДК 577.15 + 579.222.7 + + 547.262 + 547.264

ИММОБИЛИЗОВАННЫЕ ГРИБНЫЕ БИОКАТАЛИЗАТОРЫ ДЛЯ ПОЛУЧЕНИЯ КОМПЛЕКСА ЦЕЛЛЮЛАЗ, ГИДРОЛИЗУЮЩЕГО ВОЗОБНОВЛЯЕМОЕ РАСТИТЕЛЬНОЕ СЫРЬЕ

© 2013 г. **Е.Н. Ефременко**[1,2], **Н.А. Степанов**[1,2], **Д.А. Гудков**[1], **О.В. Сенько**[1], **В.И. Лозинский**[3], **С.Д. Варфоломеев**[1,2]

[1] Московский государственный университет им. М.В. Ломоносова
[2] Институт биохимической физики им. Н.М. Эмануэля РАН, г. Москва
[3] ИНЭОС РАН, г. Москва

Введение

Широко обсуждаемый сегодня процесс получения биотоплив из возобновляемого целлюлозосодержащего сырья [1—3] основан на конверсии моносахаридов, образующихся в результате ферментативной обработки исходного субстрата, прошедшего предварительную физико-химическую подготовку. Установлено, что наиболее эффективным является использование комплексов ферментов с различной гидролитической активностью, способных обеспечить комплексную и глубокую деструкцию компонентов исходного сырья с обеспечением максимального выхода моносахаров [4—5].

Наиболее эффективно действующий целлюлазный комплекс, синтезируемый и секретируемый микроскопическими грибами [6—7], как правило, содержит эндоглюканазу (EG), экзоглюканазу (CBH) и β-глюкозидазу (BG). EG расщепляет внутренние связи в молекулах целлюлозы, воздействуя на аморфные участки целлюлозных волокон. CBH атакует молекулы целлюлозы и олигосахаридов с